Efficiency of trapping processes in regular and disordered networks

A. García Cantú[1] and E. Abad[2]
[1]*Center for Nonlinear Phenomena and Complex Systems, Université Libre de Bruxelles, Brussels B-1050, Belgium*
[2]*Structural Bioinformatics and Computational Biochemistry Unit, Department of Biochemistry, University of Oxford, South Parks Road, Oxford OX1 3QU, United Kingdom*
(Received 19 October 2007; published 18 March 2008)

We use a Markov method to study the efficiency of trapping processes involving both a random walker and a deep trap in regular and disordered networks. The efficiency is gauged by the mean absorption time (average of the mean number of steps performed by the random walker before being absorbed by the trap). We compute this quantity in terms of different control parameters, namely, the length of the walker jumps, the mobility of the trap, and the degree of spatial disorder of the network. For a proper choice of the system size, we find in all cases a nonmonotonic behavior of the efficiency in terms of the corresponding control parameter. We thus arrive at the conclusion that, despite the decrease of the effective system size underlying the increase of the control parameter, the efficiency is reduced as a result of an increase of the escape probability of the walker once it finds itself in the interaction zone of the trap. This somewhat anti-intuitive effect is very robust in the sense that it is observed regardless of the specific choice of the control parameter. For the case of a ring lattice, results for the mean absorption time in systems of arbitrary size are given in terms of a two-parameter scaling function. For the case of a mobile trap, we deal with both trapping via a single channel (walker-trap overlap) and via two channels (walker-trap overlap and walker-trap crossing), thereby generalizing previous work. As for the disordered case, our analysis concerns small world networks, for which we see several crossovers of the absorption time as a function of the control parameter and the system size. The methodology used may be well suited to exploring characteristic time scales of encounter-controlled phenomena in networks with a few interacting elements and the effect of geometric constraints in nanoscale systems with a very small number of particles.

DOI: 10.1103/PhysRevE.77.031121 PACS number(s): 05.40.−a, 89.75.Hc

I. INTRODUCTION

Trapping processes play an important role in a wide variety of contexts, e.g., infectious disease propagation [1], rumor spreading in a social group [2], photon-harvesting processes in photosynthetic cells [3,4], charge carrier transport processes in polymers [5] and solids [6], or algorithms searching for similarities between the elements of a database [7].

In view of recent experimental advances, encounter-controlled processes in systems composed of a small number of units are attracting increasing interest. At a mesoscopic level, great progress has been made in the design of compartmentalized biomimetic systems with a few connected units [8] (e.g., liposome-nanotube networks) and properties reminiscent of biological cells. From a theoretical perspective, propagation phenomena in such systems give rise to simplified yet insightful coarse-grained models in terms of a few network elements with diffusion- or hopping-mediated interactions. On the other hand, design of systems with very few components at atomic length scales has nowadays become possible thanks to nanotechnological techniques that allow one to visualize and manipulate individual atoms or molecules and to control topological details [9]. The latter should be carefully designed for the specific purpose at hand (e.g., chemical reactions under nanoscale conditions in microreactors) for, as it turns out, effects arising from the discrete nature of the components, the finite size of the system, and the geometry of the substrate (e.g., impurities giving rise to spatial disorder), may have drastic effects on the kinetics.

In order to assess this kind of effects on the efficiency of trapping processes, we consider here a minimal model involving a random walker and a trap. The walker diffuses in a connected, translationally invariant network of N sites at discrete time steps, until it is instantaneously and irreversibly absorbed upon interaction with a trap initially placed at a given network site i_T. This process can be described by specifying the set of probabilities $W_{i,j}(\lambda)$ for the walker to jump from site i to a site j (for our purpose, these transition probabilities will be assumed to be functions of a certain control parameter λ). A key time scale characterizing the trapping process at hand is the mean time to absorption (MTA) τ_i given that the walker was initially placed at a site $i \neq i_T$. This set of quantities satisfies the recurrence equation [10]

$$\tau_i = \sum_k W_{i,k}(\lambda)\tau_k + 1, \quad i \neq i_T, \tag{1}$$

which expresses the Markovian character of the random walk. In principle, one need not specify the numerical value of N to find the solution of Eq. (1). However, beyond the case of simple network topologies, obtaining usable expressions in terms of an arbitrary integer N may become a rather cumbersome task. For practical purposes, one can always calculate the MTA for particular values of N by expressing Eq. (1) in matrix notation,

$$\boldsymbol{\tau} = \mathbf{W}_\lambda \boldsymbol{\tau} + \mathbf{e}, \tag{2}$$

where $\boldsymbol{\tau} = (\tau_1, \ldots, \tau_{i_T-1}, \tau_{i_T+1}, \ldots, \tau_N)^T$ is an $(N-1)$-dimensional vector, $\mathbf{e}$ is the $(N-1)$-dimensional

"one" vector $\mathbf{e}=(1,1,\ldots,1)^T$, and $\mathbf{W}_\lambda$ is the transition matrix whose entries $W_{i,j}(\lambda)$ are the jump probabilities between different network sites, each walker position corresponding to a state of the underlying absorbing Markov chain. From Eq. (3) one straightforwardly obtains the relation

$$\boldsymbol{\tau}=\boldsymbol{\Phi}_\lambda\mathbf{e}, \tag{3}$$

where

$$\boldsymbol{\Phi}_\lambda=(\mathbf{I}-\mathbf{W}_\lambda)^{-1} \tag{4}$$

is the so-called fundamental matrix.

The efficiency of a given trapping process is gauged by the average of the mean time to absorption (AMTA)—the larger the AMTA the lower the efficiency. This quantity is directly obtained by averaging the MTA over all the initial positions of the walker:

$$\langle\tau\rangle=\frac{1}{N-1}\sum_{i\neq i_T}^{N-1}\tau_i=\frac{1}{N-1}\sum_{i\neq i_T}^{N-1}\sum_j\phi_{i,j}, \tag{5a}$$

or, using (3),

$$\langle\tau\rangle=\frac{1}{N-1}\mathbf{e}^T\boldsymbol{\tau}. \tag{5b}$$

In the above setting, we have assumed that the network is translationally invariant, implying that the transient Markov states are specified by the $N-1$ relative positions of the walker with respect to the trap (if the trap is also allowed to perform jumps, the lattice site coordinates will refer to its comoving frame). In the case of networks lacking the above spatial symmetry, similar equations to the above hold, but the transient states correspond to the $N(N-1)$ nonabsorbing initial walker-trap configurations and the problem becomes much less tractable due to boundary effects. In particular, it is much harder to obtain exact solutions for arbitrary values of N in the case of a mobile trap. We shall therefore limit our full analytical description to the periodic case and use semianalytical and numerical approaches for nonsymmetric networks.

In a pioneering work [3], Montroll used the generating function method [11] to derive the result $\langle\tau\rangle=N(N+1)/6$ for an unbiased random walk on a periodic one-dimensional lattice with a single immobile trap. In what follows, we refer to this case as the classical trapping problem.

In the present work we employ the Markov method based on Eq. (1) to address extensions of the classical trapping problem, with the aim of accounting for the effects induced on the efficiency by the following processes.

(i) Walker jumps to non-nearest-neighbor sites. In Sec. II we consider the case where the walker can jump either to a first (nearest) neighbor (FN) or to a second neighbor (SN). The corresponding jump probabilities are tuned by a control parameter α.

(ii) Mobility of the trap. In Sec. III we consider a model where both the walker and the trap perform an unbiased random walk. Results for this problem have been reported for one-dimensional lattices with FN connections, assuming that absorption takes place via two channels, i.e., walker-trap overlap (WTO) through the same site occupation and walker-trap crossing (WTC) [12]. In the present work we study separately the cases where either a single channel (WTO) or two channels (WTO-WTC) are open. Furthermore, we extend results for the latter case to lattices with FN and SN connections. The WTO mechanism pertains e.g., to situations where one-dimensional (1D) displacements alternate with 3D excursions, including problems like DNA target site localization by a protein [13], while the WTO-WTC mechanism applies to quasi-1D transport processes in which a target cannot be bypassed. In the former case the MTA can be identified with the first passage time for visit to a single site, whereas in the latter case the MTA has been shown to be equivalent to a sum of conditional first passage times involving a set of sites on a modified lattice [14].

(iii) Disorder at the level of the network connections. In Sec. IV we study how the AMTA is modified by randomly creating long-range connections. In these cases, random shortcuts may be regarded as a way of mimicking spatial inhomogeneities in disordered media. In particular, shortcuts play an important role in situations such as the motion of charge carriers in entangled polymer chains [5], where jumps between spatially nearby sites can connect regions far apart along the backbone of the chain. Recently, characteristic quantities for first passage problems such as the first return time distribution [15] or the mean time to reach a particular site given an initial position [16,17] have been reported for disordered lattices. These works deal with small world (SW) network models of Newman-Watts type [18], where disorder arises by addition of connections between randomly chosen sites. These results hold for large networks and show that the mean time to reach a particular site displays monotonic behavior as a function of the disorder parameter. In contrast, here we address the behavior of the AMTA in SW networks created by the so-called Watts-Strogatz algorithm [19], where shortcuts in regular lattices are created by randomly rewiring already existing connections rather than by adding new ones. Our results show that in sufficiently small networks (a hitherto widely unexplored limit) the AMTA exhibits complex nonmonotonic behavior as a function of the disorder parameter. Finally, Sec. V is devoted to a summary of the main results.

II. EFFECT OF JUMPS TO NON-NEAREST-NEIGHBORS

Consider a system consisting of (1) a ring lattice with N sites (numbered, say, clockwise) and FN and SN site-to-site connections, (2) a walker performing unbiased jumps between connected sites, and (3) an immobile trap placed at site $i_T=N$. Let us now introduce α, a parameter restricted to the interval [0,1], controlling the relative weight of FN and SN walker jumps, respectively given by $W_{i,i\pm1}(\alpha)=(1-\alpha)/2$ and $W_{i,i\pm2}(\alpha)=\alpha/2$ (as usual, the updating of the walker position is performed modulo N). Equation (1) thus becomes

$$\tau_i=\frac{\alpha}{2}\tau_{i-2}+\frac{(1-\alpha)}{2}\tau_{i-1}+\frac{(1-\alpha)}{2}\tau_{i+1}+\frac{\alpha}{2}\tau_{i+2}+1,\quad 0<i<N. \tag{6}$$

The specific trapping mechanism is modeled by the boundary conditions, which must also reflect the lattice periodicity. In this section, we limit ourselves to the case where trapping occurs exclusively when the walker jumps on the site at which the trap is placed (WTO). This results in the boundary conditions $\tau_N=\tau_0=0$, $\tau_{-1}=\tau_{N-1}$, and $\tau_{N+1}=\tau_1$. The general solution of Eq. (6) can be constructed by adding the general solution of the corresponding homogeneous equation and a particular solution [20]. The solution obtained in this way reads

$$\tau_i = c_1 + c_2 i + c_3 \omega^i + c_4 \omega^{-i} + \frac{i^2}{3\alpha - 4}, \tag{7}$$

where $i^2/(3\alpha-4)$ is a particular solution of Eq. (6) and $\omega=[-\alpha+2+\sqrt{\alpha(4-3\alpha)}]/[2(\alpha-1)]$ is the largest root of multiplicity 1 of the characteristic polynomial associated with the corresponding homogeneous equation. The coefficients in (7) are easily found to be $c_1=G\omega(\omega^N+1)$, $c_2=N/(4-3\alpha)$, $c_3=G\omega$, and $c_4=-G\omega^{N+1}$, where $G=2N/[(4-3\alpha)(\omega^2-1)(1-\omega^N)]$.

Inserting (7) in (5a), the AMTA can be expressed in terms of Montroll's result as

$$\langle \tau \rangle = \frac{N(N+1)}{6}\Omega(\omega,N), \tag{8}$$

where the scaling function $\Omega(\omega(\alpha),N)$ reads

$$\Omega(\omega,N) = \frac{N^2(1+\omega+\omega^2)}{(N^2-1)(\omega-1)^4}\left((\omega-1)^2 + \frac{12\omega(1+\omega^N)(\omega-1)}{N(1-\omega^N)(\omega+1)} - \frac{1-14\omega+\omega^2}{N^2}\right). \tag{9a}$$

In the limit $\alpha\to 1/2$ (FN and SN jumps take place with the same probability), Eq. (9a) yields the formula

$$\langle \tau \rangle = \frac{N^3}{15(N-1)}\left(1 - \frac{17}{5N^2} + \frac{12\sqrt{5}}{5N}\frac{1+\left(\frac{-3+\sqrt{5}}{2}\right)^N}{1-\left(\frac{-3+\sqrt{5}}{2}\right)^N}\right). \tag{9b}$$

Equations (8) and (9a) were first obtained by Lakatos-Lindenberg and Shuler [21] by means of the generating function method.[1] However, they did not discuss in detail the behavior of $\Omega(\omega(\alpha),N)$ as a function of α, which we aim to do in the following.

A plot of $\Omega(\omega,N)$ vs α, Fig. 1, shows that the behavior of $\langle\tau\rangle$ depends on the parity of N. For even values of $N>2$ expression (9a) and (9b) displays a minimum in the α interval (0,1) and diverges as $\alpha\to 1$ [see Fig. 1(a)]. The minimum arises from the interplay of two competing effects. (a) When α is increased, with a high probability the walker attains the neighborhood of the trap in fewer steps. Therefore, in the weak-α region the AMTA must decrease with increasing α. (b) In the limit $\alpha\to 1$ any walk will diffuse through either of two disconnected topological cycles depending on the initial condition; one cycle consisting of sites labeled with even numbers and the other one with odd-numbered sites only. Clearly, the walker will never be trapped if the cycle dictated by the initial condition does not include the trapping site i_T.

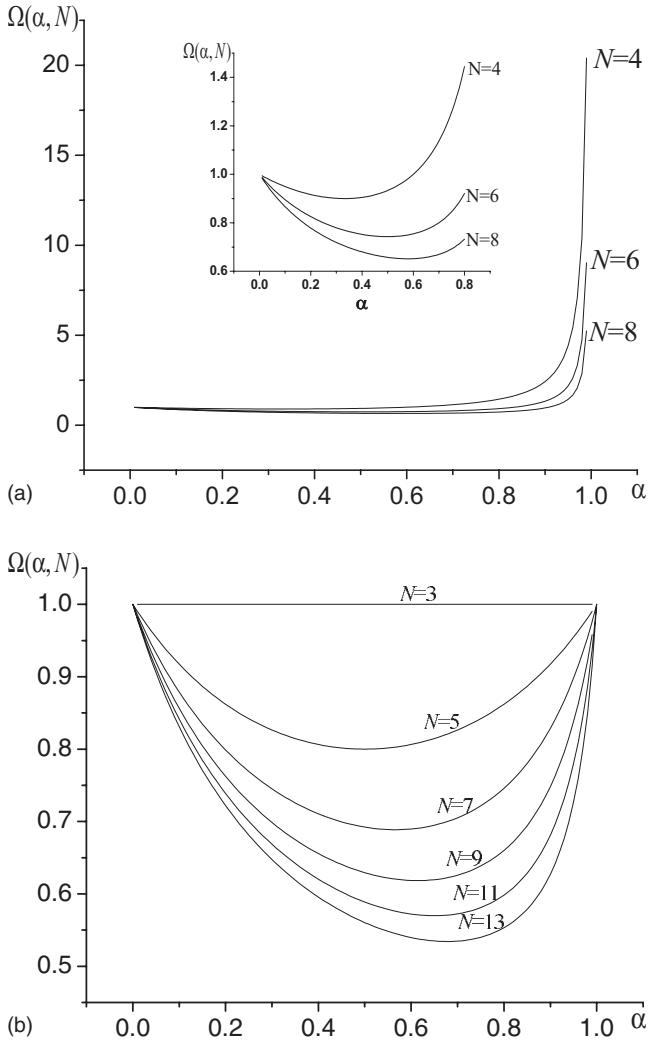

FIG. 1. $\Omega(\omega(\alpha),N)$ vs α, for (a) even and (b) odd N.

In contrast, if N is odd, the walker will visit all lattice sites regardless of its initial position and trapping will be guaranteed. As in the even-lattice case, Ω displays a minimum for a value $0<\alpha_{\min}<1$ provided that $N>3$ [see Fig. 1(b)], and Montroll's result is recovered from expression (8) for both $\alpha\to 0$ and $\alpha\to 1$, i.e., $\lim_{\alpha\to 0,1}\Omega(\omega(\alpha),N_{\text{odd}})=1$ (for $N=3$ one actually has $\Omega=1$ for all values of α). In this case effect (a) still holds, but effect (b) is no longer present. Instead, one has a new effect (c) by which the limit $\alpha\to 1$ brings one again closer to the $\alpha=0$ case, as the length of the cycle involving SNs only is equal to the length of the cycle involving FNs only (a cycle of length N); see Fig. 2

Thus, the AMTA for $\alpha=1$ must be the same as for $\alpha=0$ and the combination of (a) and (c) by continuity implies that there must be a minimum for an intermediate value

[1] In their paper, the result (9a) was expressed in terms of both ω (termed X there) and α. However, the factor ω appearing in the numerator of the second term in the brackets was omitted due to a misprint.

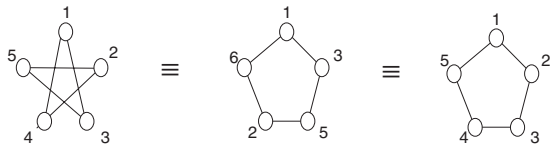

FIG. 2. Equivalence between FN and SN cycles in periodic one-dimensional lattices.

$0<\alpha_{\min}<1$ [Fig. 1(b)]. As the value of N increases, effect (a) clearly becomes dominant, implying that $\alpha_{\min}\to 1$ as $N\to\infty$.

III. CASE OF A MOVING TRAP

Let us now turn to the situation where, in addition to the walker, the trap is also allowed to perform unbiased random jumps between connected sites. At each time step, the walker always jumps, whereas the trap will be assumed to jump clockwise or counterclockwise with probability p or to remain immobile with probability $1-p$. Thus, p plays the role of a control parameter which tunes the synchronicity in the walker-trap motion. In what follows we shall focus on the behavior of the AMTA as a function of p and N, for the separate cases where trapping takes place via WTO and WTO-WTC. The problem is most easily solved by switching to a comoving-frame representation.

A. Ring lattice with first-neighbor connections

The passage to a comoving-frame representation is schematically depicted in Fig. 3. In this representation the trap is assumed to be fixed, while the walker performs jumps of variable length Δ. The value of Δ is given by the change in the trap-walker distance (measured in lattice spacings) after each joint diffusion event. The underlying trapping process can be regarded as an absorbing chain whose single-step transition probabilities are shown in Table I

The Markov states i refer to the positions of the walker with respect to the comoving frame where the trap is immobile (in agreement with the convention used in the previous section, the trap is assumed to be at site $i_T=N$). Thus, the MTA obeys the equation

$$\tau_i=\frac{p}{4}\tau_{i-2}+\frac{(1-p)}{2}\tau_{i-1}+\frac{p}{2}\tau_i+\frac{(1-p)}{2}\tau_{i+1}+\frac{p}{4}\tau_{i+2}+1,\quad 0<i<N, \tag{10}$$

with solutions of the form

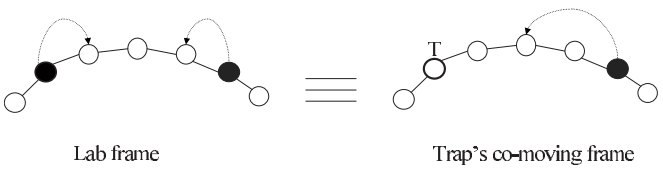

FIG. 3. Synchronous jump event in both the laboratory frame and the trap's comoving frame.

TABLE I. Transition probabilities for the case with FN connections.

$\Delta=$	0	1	2
$W_{i,i\pm\Delta}(p)=$	$p/4$	$(1-p)/2$	$p/4$

$$\tau_i=c_1+c_2+c_3\xi^i+c_4\xi^{-i}-\frac{i^2}{1+p}, \tag{11}$$

where $\xi=(-1+\sqrt{1-p^2})/p$ (thus, ξ decreases from 0 to -1 as p increases from 0 to 1). The boundary conditions of Eq. (10) are again dictated by the lattice periodicity and the trapping mechanism under consideration.

1. Trapping via walker-trap overlap

Assuming that a trapping event occurs exclusively through WTO, the boundary conditions of Eq. (10) are the same as for Eq. (6). Proceeding as in the previous case, one obtains straightforwardly the result

$$\langle\tau\rangle=\frac{N(N+1)}{6}\Psi(\xi,N), \tag{12}$$

where the scaling function reads

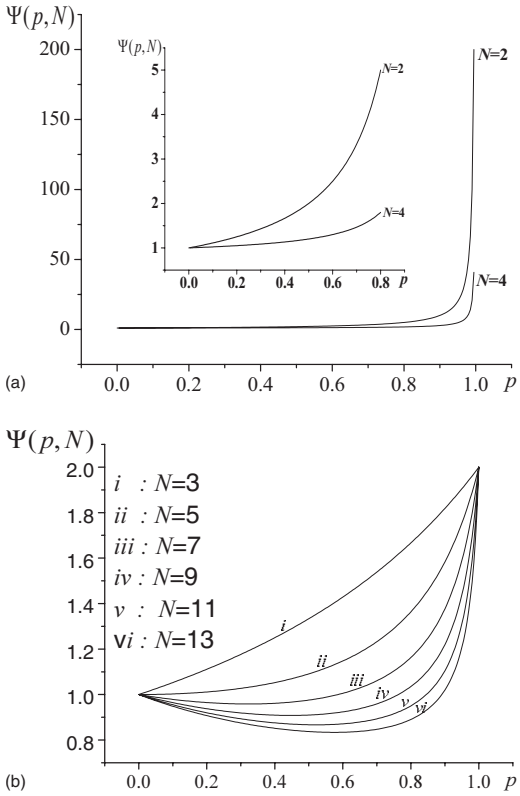

FIG. 4. $\Psi(\xi(p),N)$ vs p, for (a) even N (for $N>6$ the plots for different values of N become practically indistinguishable) and (b) odd N.

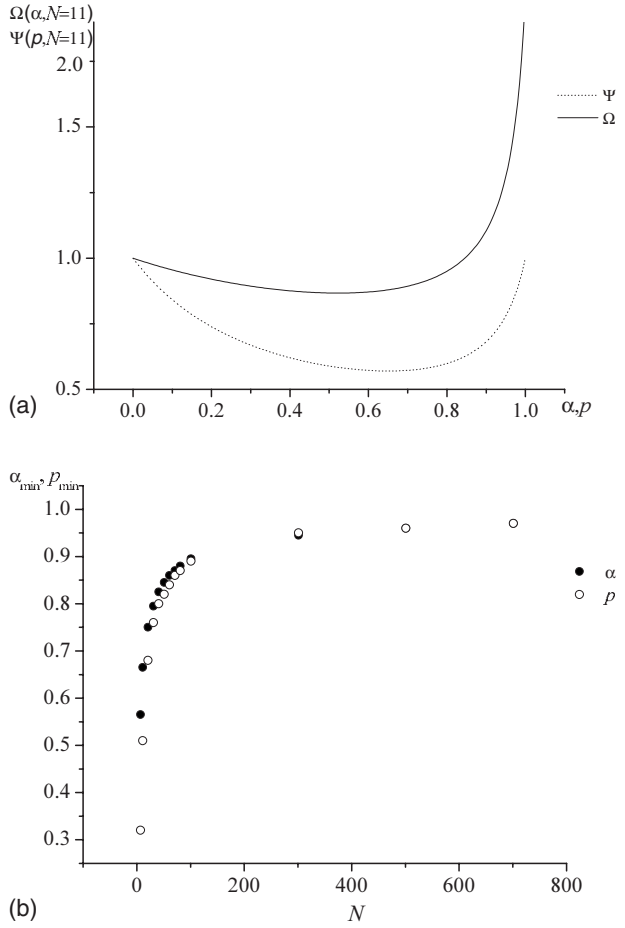

FIG. 5. Comparative plots of (a) $\Psi(\xi(p),N)$ and $\Omega(\omega(\alpha),N)$ as functions of p and α, respectively, and (b) $p_{\min}$ and $\alpha_{\min}$ as functions of N. The values of $p_{\min}$ and $\alpha_{\min}$ have been obtained by setting the derivatives of the scaling functions (13) and (9a) equal to zero.

$$\Psi(\xi,N)=\frac{N^2(1+\xi^2)}{(N^2-1)(\xi-1)^4}\left((\xi-1)^2+\frac{12\xi(1+\xi^N)(\xi-1)}{N(1-\xi^N)(\xi+1)}-\frac{1-14\xi+\xi^2}{N^2}\right). \tag{13}$$

In the comoving-frame representation, the parameter p plays a similar role as α in the process described in Sec. II, i.e., controlling the length Δ of the walker jumps. For $p=0$, only FN jumps ($\Delta=1$) occur, while for $p=1$ the walker either remains immobile or it jumps to a SN ($\Delta=0,2$). Notice the similarity between expressions (13), (9a), and (9b). It is therefore no surprise that, as the degree of synchronicity is increased, the two-walker system with WTO displays the same kind of parity effect as the one observed in Sec. II. The behavior of the scaling function (13) is displayed in Fig. 4. For an even value of N, $\Psi(\xi,N)$ diverges as $p\to 1$ [Fig. 4(a)]. Again, this results from the fact that, for some initial configurations, the walker and the trap will never meet if they move fully synchronously. On the other hand, for lattice sizes $N=3,5$ $\Psi(\xi,N)$ increases monotonically with p [Fig. 4(b)]. This can be understood by noting that in very small

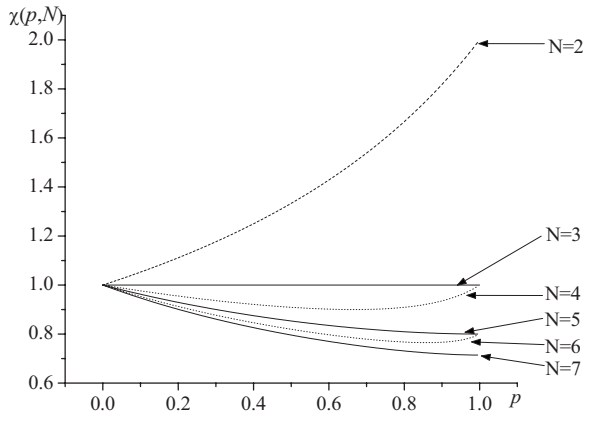

FIG. 6. $\chi(\xi(p),N)$ as a function of p.

lattices the walkers are always in a *preabsorbing* configuration, i.e., in positions for which absorption can take place within a single step. However, the probability of noninteraction increases with p. For instance, for $N=3$ the probability that the walker survives after a single step is $(2+p)/4$. Therefore, one expects that the efficiency is maximal for purely asynchronous motion ($p=0$). A similar argument applies to the $N=5$ case. For odd lattices of size $N>5$, $\Psi(\xi,N)$ displays a minimum for a value $0<p_{\min}<1$ [Fig. 4(b)]. As in the case treated in Sec. II, for sufficiently large lattices the AMTA (12) decreases with increasing p in the region of small p values. Therefore, understanding the origin of this minimum amounts to understanding why the AMTA increases as the value of p becomes close to 1.

This increase can be explained as follows: at $p=1$, the AMTA is given by the sum of the mean number of steps of length $\Delta=2$, which we denote by $\langle T\rangle_{\Delta=2}$, plus the mean number of steps of length $\Delta=0$, $\langle T\rangle_{\Delta=0}$. By virtue of the argument shown in Fig. 2, one has $\langle\tau\rangle_{p=0}=\langle T\rangle_{\Delta=2}$; on the other hand, since jumps of lengths $\Delta=0$ and 2 occur with equal probability, one concludes that $\langle T\rangle_{\Delta=2}=\langle T\rangle_{\Delta=0}$. This result also confirms that the purely synchronous case is twice less efficient than the synchronous one [see Fig. 4(b)].

Alternatively, one can gain insight into the behavior of the efficiency by studying how increasing the parameter p affects the number of preabsorbing configurations, as well as the probability that a preabsorbing configuration leads to trapping. Both aspects are contained in the (initial-condition-averaged) probability P_{abs} that the walker gets trapped in a single step (clearly, the efficiency increases with P_{abs}). For a ring of odd size N this quantity reads

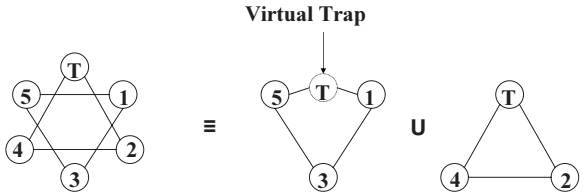

FIG. 7. Decomposition of an $N=6$ lattice with connections to SNs only into two disconnected cycles. The cycle with even sites includes the real trap, whereas the cycle with odd sites contains a virtual trap.

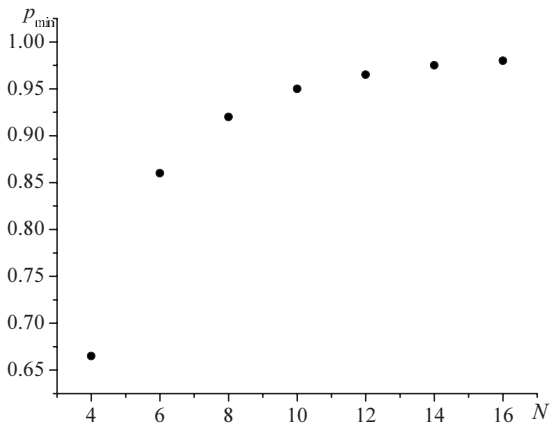

FIG. 8. $p_{\min}$ vs N for the case of WTO-WTC trapping. The value of $p_{\min}$ is computed by setting the derivative of the scaling function (17) equal to zero.

$$P_{\text{abs}} = \frac{(2-p)}{2(N-1)}. \tag{14}$$

Expression (14) shows that the walker-trap encounter probability diminishes with increasing p. Therefore, one can interpret the origin of the minimum as arising from the competition between the enhancement of relative diffusion (a reduction of the effective size of the lattice) and the decrease of P_{abs}. In Fig. 4(b) one observes that the minimum position $p_{\min}$ shifts toward $p=1$ as $N\to\infty$; this clearly results from the fact that P_{abs} loses importance as N increases.

It is worth comparing the present case with the one of Sec. II. Figure 5(a) displays plots of the scaling functions Ω vs α and Ψ vs p. This figure shows that the trapping efficiency is more enhanced by allowing for non-nearest-neighbor jumps while keeping the trap fixed than by allowing the trap to move while restricting the walker jumps to FNs. Clearly, this difference arises from the fact that in the latter case the distance separating the walker from the trap remains unchanged after a jump event with a nonzero probability ($P_{\Delta=0}=p/2$). However, in the limit of large lattices the behavior of the efficiency becomes increasingly similar, as shown in Fig. 5(b).

2. *Trapping via walker-trap overlap and walker-trap crossing*

Recently, Abad *et al.* [12] have treated this case by means of the difference equation approach, providing results for the AMTA in the limiting case $p=1$,

TABLE II. Transition probabilities for the case with FN and SN connections.

$\Delta=$	0	1	2	3	4
$W_{i,i\pm\Delta}(p)=$	$p/4$	$(2-p)/8$	$(4-3p)/16$	$p/8$	$p/16$

$$\langle\tau\rangle = \begin{cases} \dfrac{N(N+1)(N+1)}{12(N-1)} & \text{for } N \text{ even}, \\ \dfrac{(N+1)(N+3)}{12} & \text{for } N \text{ odd}, \end{cases} \tag{15}$$

as well as results for arbitrary values of p and small N values. In Ref. [12], an interpretation of this trapping problem in terms of a generalized ruin problem was also provided. We now revisit this problem with the aim of deriving general expressions in N and p.

Incorporating WTC amounts to considering that, in addition to WTO, clock- or counterclockwise jumps across the trap lead to absorption. Trapping through the WTO and WTC channels is expressed via the boundary conditions $\tau_{-1}=0$, $\tau_0=0$, $\tau_N=0$, and $\tau_{N+1}=0$. The AMTA is found to be

$$\langle\tau\rangle = \frac{N(N+1)}{6}\chi(\xi,N), \tag{16}$$

where the scaling function reads

$$\chi(\xi,N) = \frac{(1+\xi^2)}{(N-1)(\xi-1)^4}\left(N(\xi-1)^2 + \frac{(\xi^4-1)(1+\xi^{N+1})}{(1+\xi^2)(1-\xi^{N+1})} + 2\xi\frac{2N(\xi-1)(1+\xi^N)+3(1+\xi)(1-\xi^N)}{N(1-\xi^{N+1})}\right). \tag{17}$$

The main effect introduced by WTC is that, in contrast with previous cases, absorption occurs regardless of the walker's initial position and the value of the control parameter p. As it turns out, the $p=1$ limit of (17) is consistent with Eqs. (15).

The plot $\chi(\xi(p),N)$ vs p, Fig. 6, exhibits a kind of parity effect different from the one arising from the scaling functions defined in (9a) and (13). The case $N=2$ is the only one for which χ increases monotonically with p. For even lattices with $N\geq 4$, χ attains a minimum for an intermediate value of p, as observed for odd lattices in the cases described by the scaling functions (9a) and (13). In contrast, for odd lattices with $N>3$, the scaling function χ decreases monotonically with increasing p. When $N=3$, as in (9a), χ remains constant in the interval [0,1], $\chi(p)=1$.

In the $N=2$ case the spatially averaged one-step absorption probability is $P_{\text{abs}}=(2-p)/4$, which explains the fact that the purely asynchronous case $p=0$ is the most efficient one. On the other hand, for $N>2$ one has $P_{\text{abs}}=1/(N-1)$, i.e., it no longer depends on p. However, if N is even, in the limiting case $p=1$ the walker can be absorbed only via one of the two channels, either WTO or WTC; the selected channel will depend on the parity of the initial walker-trap separation. In the trap's comoving frame the walker is absorbed by the trap if it moves on the cycle of even sites, or it is absorbed by a virtual trap[2] (corresponding to trapping via WTC) if it moves along the "odd" cycle (see the example in Fig. 7 for the $N=6$ case).

[2]The virtual trap captures the walker for any transition from site 1 to $N-1$ or backward.

TABLE III. Analytical expressions plotted in Fig. 9(b).

N	$\langle\tau\rangle_p$
10	$\frac{2}{99}\frac{275p^3-3020p^2-12400p+35264}{5p^3-20p^2-16p+64}$
11	$\frac{-176}{445}\frac{123p^4-1520p^3+48p^2+21824p-33536}{p^5-28p^4+208p^3-320p^2-512p+1024}$
12	$\frac{4}{11}\frac{9p^3-70p^2-128p+656}{p^3-6p^2+16}$
13	$\frac{-104}{699}\frac{177p^5+5836p^4-44336p^3+9792p^2+344064p-467968}{p^6-20p^5-128p^4+1216p^3-1792p^2-2048p+4096}$
14	$\frac{14(2639p^6-18872p^5-569072p^4-3531136p^3-1005568p^2-21268480p+27561984)}{4901(7p^7-56p^6-112p^5+1408p^4-2048p^3-2048p+4096)}$

Thus, for even lattices the case of fully synchronous motion cannot be the most efficient one, as there is only one absorption channel effectively active for a given initial condition. This explains that the minimum of the AMTA is observed for a value $p=p_{\min}$ between 0 and 1. In contrast, if the lattice is odd, both channels are simultaneously active regardless of the value of p and the initial two-walker configuration. The plot $p_{\min}$ vs N, Fig. 8, shows that with increasing lattice size N the minimum of $\chi(\xi,N)$ shifts toward $p=1$ faster than in the previous cases depicted in Fig. 5(b), where only WTO was active.

In order to find how $p_{\min}$ approaches 1 with increasing system size N, we expand the scaling function $\chi(\xi,N)$ in a Taylor series about $\xi=-1$ (which corresponds to the limiting value of $p_{\min}$ for very large systems). This series will be a good approximation for values of ξ close to -1, and in particular for $\xi_{\min}=(-1+\sqrt{1-p_{\min}^2})/p_{\min}$, which gets close to -1 for a sufficiently large value of N. To lowest order of accuracy, we keep just as many terms in the expansion as necessary to observe a local minimum of $\chi(\xi,N)$ as a function of ξ. As it turns out, one must retain terms up to fourth order, resulting in the expression

$$\chi(\xi,N) \approx 2\alpha - \alpha(\xi+1)^2 - \alpha(\xi+1)^3 + \beta(\xi+1)^4, \quad (18)$$

where $\alpha=\frac{1}{4}\frac{N+2}{N-1}$ and $\beta=\frac{1}{32}\frac{(N+4)(N+2)(N-2)}{N-1}$. One now requires that at $\xi=\xi_{\min}$ the AMTA display a minimum, i.e.,

$$\left.\frac{\partial\chi(\xi,N)}{\partial\xi}\right|_{\xi=\xi_{\min}} = 0, \quad (19)$$

leading to

$$4\beta(\xi_{\min}+1)^3 - 3\alpha(\xi_{\min}+1)^2 - \alpha(\xi_{\min}+1) = 0. \quad (20)$$

This equation has two solutions, namely,

$$\xi_{\min}+1 = \frac{3\varepsilon}{8} \pm \sqrt{\frac{9}{64}\varepsilon^2+\frac{1}{2}\varepsilon}, \quad (21)$$

where $\varepsilon=\alpha/\beta$. As the $-$ sign corresponds to an unphysical value $\xi_{\min}<-1$, we choose the $+$ sign. A series expansion of the right-hand side (RHS) of Eq. (21) in powers of N^{-1} yields

$$\xi_{\min}+1 = \frac{2}{N} + O(N^{-2}). \quad (22)$$

Expressing $p_{\min}$ in terms of $\xi_{\min}$, one gets

$$1-p_{\min} = \frac{(1+\xi_{\min})^2}{1+\xi_{\min}^2} \approx \frac{(1+\xi_{\min})^2}{2} = \frac{2}{N^2} + O(N^3). \quad (23)$$

Finally, inserting Eq. (23) back into (16), one gets

$$\langle\tau\rangle_{p=1} - \langle\tau\rangle_{p=p_{\min}} = \frac{1}{6} + O(N^{-1}). \quad (24)$$

B. Ring lattice with first- and second-neighbor connections

Let us now address the case in which both the walker and the trap perform symmetric jumps to FNs and SNs, whereby at each time step the walker always jumps and the trap jumps only with probability p. In the trap's comoving frame, the walker can now perform jumps of lengths $\Delta=0,1,2,3,4$. As it turns out, the procedure described in the previous sections gives a higher-order difference equation, leading to cumbersome expressions for the roots of the associated characteristic polynomial. Instead, we limit ourselves to treating this problem for particular values of N by means of the fundamental matrix method, summarized by expressions (3), (4), and (5b). The absorbing Markov chain in this case will be described by the single-step probabilities for the possible jumps in the comoving frame. For lattice sizes $N>8$, these probabilities are shown in Table II. The absorbing states of the chain are specified by the trapping mechanism under consideration.

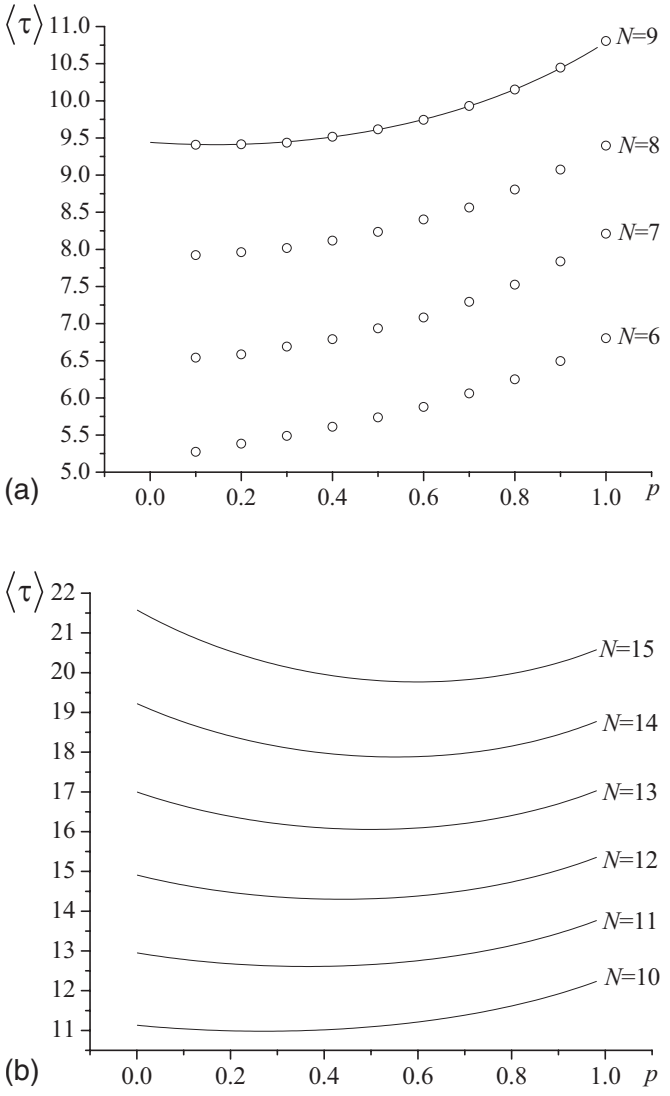

FIG. 9. $\langle\tau\rangle$ vs p: (a) Monte Carlo simulation results (dots) for $N \leq 9$ and (b) theoretical results (solid line) for $N > 9$. Case of FN and SN connections with WTO trapping.

For lattices of size $N \leq 8$ the jump probabilities are no longer given by the formulas in Table II due to the fact that a long jump away from the trap may *reduce* the walker distance because of the lattice periodicity.

1. Trapping via walker-trap overlap

In this case the corresponding absorbing chain has a single absorbing state (corresponding to trapping at site i_T). We construct the associated fundamental matrix $\mathbf{\Phi}_p$ [cf. Eq. (4)] for different lattices sizes $N \geq 9$, and we then obtain the AMTA by applying formulas (3) and (5b). For lattices with $N < 10$ we estimate the AMTA by means of Monte Carlo simulations. Analytical results obtained for different values of N are displayed in Table III and plotted in Figs. 9(a) and 9(b) together with simulation results for smaller lattices.

TABLE IV. Slope values for $N > 13$.

N	$d\langle\tau\rangle_{\text{nonint}}/dp\|_{p=0}$
14	−0.796422
15	−1.22366
16	−1.72703

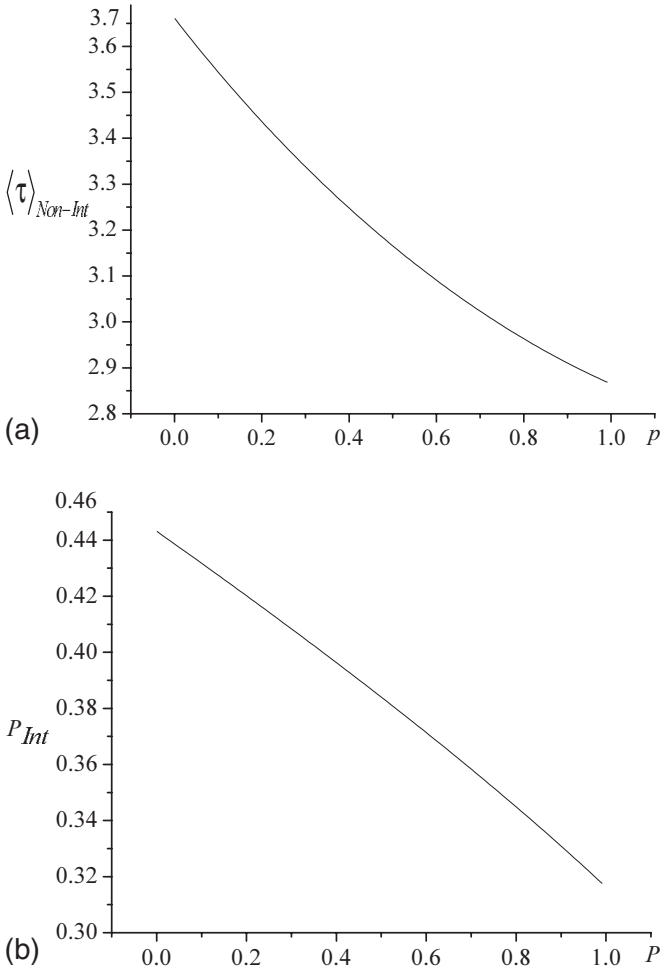

FIG. 10. (a) $\langle\tau\rangle_{\text{nonint}}$ and (b) P_{int} vs p, both for $N=13$.

One observes that the even-odd effect described in Sec. III A is suppressed. For $N < 10$ the AMTA increases monotonically with p [Fig. 9(a)]. This can be understood by noting that in these cases any site is preabsorbing, i.e., trapping is always possible within a single time step. As explained in Sec. III A for the case with WTO only, the probability P_{abs} of absorption in one step once the walker and the trap are found in the *interaction zone*[3] decreases as p increases [e.g., $P_{\text{abs}} = (16-5p)/112$ for a lattice with $N=8$] and trapping is delayed.

For $N > 9$ the AMTA exhibits a minimum within the interval (0,1); Fig. 9(b). This minimum arises from competing phenomena associated with two different characteristic quantities as follows.

(a) The mean time $\langle\tau\rangle_{\text{nonint}}$ needed by the walker to reach the interaction zone. The lower this quantity, the lower the

[3]Hereafter we shall term "interaction zone" the set of all preabsorbing sites around the trap.

TABLE V. Results obtained for the case with FN and SN connections and WTO-WTC trapping.

N	$\langle\tau\rangle_p$
10	$\frac{32}{7}\frac{90p^4-1109p^3-5726p^2-42532p+55264}{9p^5+44p^4-3060p^3+9344p^2-4352p-22784}$
11	$\frac{2(3479p^4-21056p^3-43232p^2+378496p-470016)}{251p^5-374p^4-11936p^3+34848p^2+14080p-73728}$
12	$\frac{8}{9}\frac{9151p^5-262060p^4+1203440p^3+1151360p^2-13057280p+15628288}{341p^6-8724p^5+15280p^4+180800p^3-510720p^2-182272p+954368}$
13	$\frac{64}{5}\frac{3753p^5-58326p^4+230608p^3+98976p^2-1714816p+1990912}{2207p^6-27128p^5+47632p^4+335104p^3-922880p^2-294912p+1544192}$
14	$\frac{4}{11323}\frac{15717p^6-858276p^5+11285296p^4-40943232p^3-5396736p^2+225734656p-255447040}{p^7-14912p^6+143400p^5-247808p^4-1222144p^3+3298816p^2+954368p-4997120}$

AMTA. In the trap's comoving frame $\langle\tau\rangle_{\text{nonint}}$ is easily computed by regarding all the preabsorbing sites around i_T as absorbing states. One then constructs the fundamental matrix $\mathbf{\Phi}_{\text{nonint}}$ corresponding to the walker transitions between sites outside the interaction zone. The AMTA obtained from this fundamental matrix via Eq. (5b) can then be identified with $\langle\tau\rangle_{\text{nonint}}$.

(b) The probability that absorption occurs once the walker enters the interaction zone, P_{int}. Clearly, the higher P_{int}, the lower the AMTA. In order to calculate P_{int} one first computes the fundamental matrix $\mathbf{\Phi}_{\text{int}}$, associated with the interaction zone. This can be done similarly as for $\mathbf{\Phi}_{\text{nonint}}$, now assuming that in addition to the trap all the sites outside the interaction zone are absorbing. The probabilities of absorption are given by the matrix [10]

$$\mathbf{B} = \mathbf{\Phi}_{\text{int}}\mathbf{R}_{\text{int}}, \tag{25}$$

where $\mathbf{R}_{\text{int}}$ denotes the matrix whose entries $R_{i,j}$ are the transition probabilities from the preabsorbing to the absorbing sites. The i,j entry of $\mathbf{B}$ provides one with the probability that the walker be absorbed at site j given that it started its walk from site i. The probability P_{int} is thus given by the average

$$P_{\text{int}} = \frac{1}{N_{\text{int}}}\sum_{\{K\}_{\text{int}}} B_{K,i_T} \tag{26}$$

with N_{int} denoting the number of elements of the set of preabsorbing sites $\{K\}_{\text{int}}$.

Figure 10 displays the plots $\langle\tau\rangle_{\text{nonint}}$ vs p and P_{int} vs p obtained for $N=13$. As expected, it shows that for sufficiently large lattices the mean time to reach the interaction zone decreases monotonically with increasing p [Fig. 10(a)]. However, the probability that the walker is absorbed by the trap instead of escaping the interaction zone also decreases monotonically with increasing p [Fig. 10(b)]. The presence of these two competing effects explains the nonmonotonic behavior of the AMTA for large lattices. Furthermore, the function P_{int} becomes independent of N for lattice sizes $N \geq 13$. In this case P_{int} reads

$$P_{\text{int}} = \frac{1}{4}\frac{12\,480 - 11\,504p + 2976p^2 - 129p^3 - 11p^4}{p^4 + 60p^3 + 600p^2 - 4688p + 7040}, \tag{27}$$

$$N \geq 13.$$

Thus, the mean time spent by the walker in the interaction zone, given that it is eventually trapped, no longer depends on N and is a monotonically increasing function of p. In contrast, the slope $\frac{d\langle\tau\rangle_{\text{nonint}}}{dp}$ becomes increasingly negative for $N>13$; see Table IV.

Since in this regime the decrease of $\langle\tau\rangle_{\text{nonint}}$ with increasing p gets steeper with increasing N, while the time spent in the interaction zone remains constant, one concludes that the contribution to the AMTA of transitions between states out of the interaction zone dominates in large lattices. Therefore, in these cases the purely synchronous case is more efficient than the purely asynchronous one [see Fig. 9(b) for $N=15$] and one expects that in the limit $N\to\infty$ the AMTA will decrease monotonically with p.

2. Trapping via walker-trap overlap and walker-trap crossing

Incorporating WTC amounts to assuming that transitions with $\Delta=2,3,4$ across the trap lead to absorption. Some Markov results for the AMTA are given in Table V and plotted in Fig. 11. They are compatible with the limiting expressions obtained in [22] for the $p=1$ case. In all cases the totally synchronous case is the most efficient one since, as opposed to the case with FN connections only, both trapping channels are now accessible for any value of p and N.

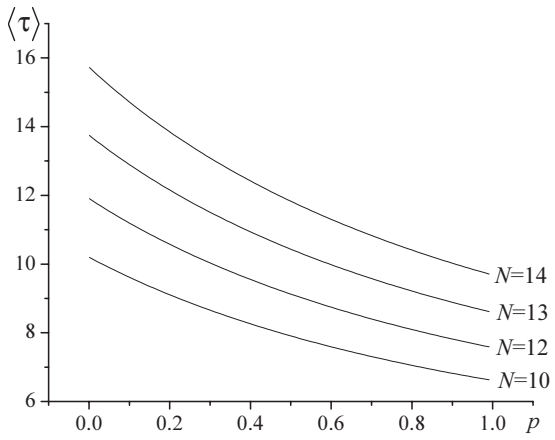

FIG. 11. $\langle \tau \rangle$ vs p, for $9 < N < 15$. Case of FN and SN connections and WTM-WTC trapping.

IV. THE TRAPPING PROBLEM IN SMALL WORLD NETWORKS

In this section we study the efficiency of the classical trapping problem on a Watts-Strogatz SW (WSSW) network [19]. We shall consider the case of a WSSW network constructed from a ring lattice with FN and SN connections by randomly rewiring links with probability ρ. We shall adopt a so-called quenched disorder approach [23] in which the efficiency will be characterized by the average of the AMTA over an ensemble of WSSW realizations. In the previous cases we calculated the AMTA by taking the average of the MTAs needed for the walker to reach the fixed trap at site i_T. In the case of SW networks the spatial symmetry is lost. The number of Markov states increases dramatically, as their characterization now requires binary sets of walker-trap configurations rather than a single coordinate. Calculating the AMTA for a SW network requires averaging the MTA over $N(N-1)$ nonabsorbing walker-trap configurations. For the present case the fundamental matrix method as formulated above requires specification of an absorbing chain for each trap position and thus inversion of N matrices of size $(N-1)\times(N-1)$ [cf. Eq. (4)]. Instead, we shall apply the method of the *pseudoinverse* of the Laplacian matrix, which allows one to determine the AMTA directly from the network topology and requires inversion of a single $N \times N$ matrix. In general, the Laplacian matrix of a network is defined as

$$L_{i,j} = \begin{cases} w_{i,j}, \quad i \neq j, & \text{if nodes } i \text{ and } j \text{ are connected,} \\ -\sum_{k \neq i} w_{i,k} & \text{if } i = j, \\ 0 & \text{otherwise,} \end{cases} \tag{28}$$

where $w_{i,j}$ denote the weights of connections (in our case $w_{i,j}=1, \ \forall \ i,j$). Given a regular network of N elements, the pseudoinverse of the corresponding Laplacian matrix is [24]

$$\mathbf{L}^{\dagger} = \left(\mathbf{L} - \frac{\mathbf{e}\mathbf{e}^T}{N} \right)^{-1} + \frac{\mathbf{e}\mathbf{e}^T}{N}. \tag{29}$$

If the network is connected, its associated pseudoinverse matrix (29) is well defined and the elements $l^{\dagger}_{i,j}$ are related to the mean time for a walker to reach a node j starting from an initial position i as follows [7]:

$$\tau_{i,j} = \sum_{k=1}^{N} (l^{\dagger}_{i,k} - l^{\dagger}_{i,j} - l^{\dagger}_{j,k} + l^{\dagger}_{j,j}) d_{k,k} \tag{30}$$

where $d_{k,k}$ denotes the k element of the diagonal of $\mathbf{L}$. The AMTA then reads

$$\langle \tau \rangle = \frac{1}{N(N-1)} \sum_{i \neq j} \sum_{j=1}^{N} \tau_{i,j}. \tag{31}$$

For a given value of ρ, we consider the average of (31) over an ensemble of SW networks of equal size N, hereafter denoted by $\langle\langle \tau \rangle\rangle_{\rho}$.

Figure 12 displays the plot $\langle\langle \tau \rangle\rangle_{\rho}$ vs ρ for different sizes N, obtained by applying Eqs. (30) and (31) to an ensemble of 1×10^4 WSSW network realizations, as well as Monte Carlo simulation results for an equivalent ensemble of the same size. For $N < 12$, $\langle\langle \tau \rangle\rangle_{\rho}$ has a maximum $\rho_{\max}$ within the interval (0,1), and the highest efficiency is attained in the totally ordered case [Figs. 12(a)–12(d)]. For $N \geq 12$, $\langle\langle \tau \rangle\rangle_{\rho}$ displays both a minimum and a maximum, at values $\rho_{\min}$ and $\rho_{\max}$, respectively [Figs. 12(e) and 12(f)]. As N becomes larger, one observes that the maximum begins to flatten out.

In order to gain insight into the behavior of $\langle\langle \tau \rangle\rangle_{\rho}$ vs ρ, it is useful to recall the behavior of the diameter and the mean clustering coefficient (MCC) in a WSSW network [19]. When ρ is increased the diameter quickly falls toward a minimum value, asymptotically attained as ρ approaches 1. In contrast, the slope of the MCC remains very low up to relatively large values of ρ, and drops to zero as $\rho \to 1$. This induces two competing effects ruling the behavior of $\langle\langle \tau \rangle\rangle_{\rho}$.

(i) On the one hand, the decrease of the effective network size (diameter) with increasing ρ implies that fewer jumps are necessary for the walker to reach the interaction zone. In principle, this enhances the efficiency of trapping.

(ii) On the other hand, when ρ is close to 1, the MCC vanishes and the walker delocalizes: jumps to nearest neighbors are hindered and jumps to farther nodes are strongly favored. Clearly, delocalization hinders trapping whenever the walker is at a short Euclidean distance from the trap.

In WSSW networks of small sizes, $N < 12$, the effective size is already extremely small due to SN connections. Hence, effect (i) becomes irrelevant compared with effect (ii). As a consequence $\langle\langle \tau \rangle\rangle_{\rho}$ grows monotonically with ρ, attaining a maximum at $\rho_{\max}$ [Figs. 12(a)–12(d)]. Since the MCC equals zero for $\rho=1$, one naturally inquires why $\rho_{\max} \neq 1$. This can be explained by the fact that for $\rho=1$ the network becomes fully disordered and the interaction zone fully sparse. Therefore, although the MCC is zero, the trap is reached in fewer steps. On the other hand, in WSSW networks a short diameter can coexist with a relatively high MCC [19]. This ensures the coexistence of effects (i) and (ii). As a consequence, in the case of larger sizes, $N \geq 12$, these effects compensate each other, giving rise to a minimum of $\langle\langle \tau \rangle\rangle_{\rho}$ at $\rho_{\min}$ [Figs. 12(e) and 12(f)]. Clearly, for very large networks, $N \gg 1$, effect (i) prevails over effect (ii).

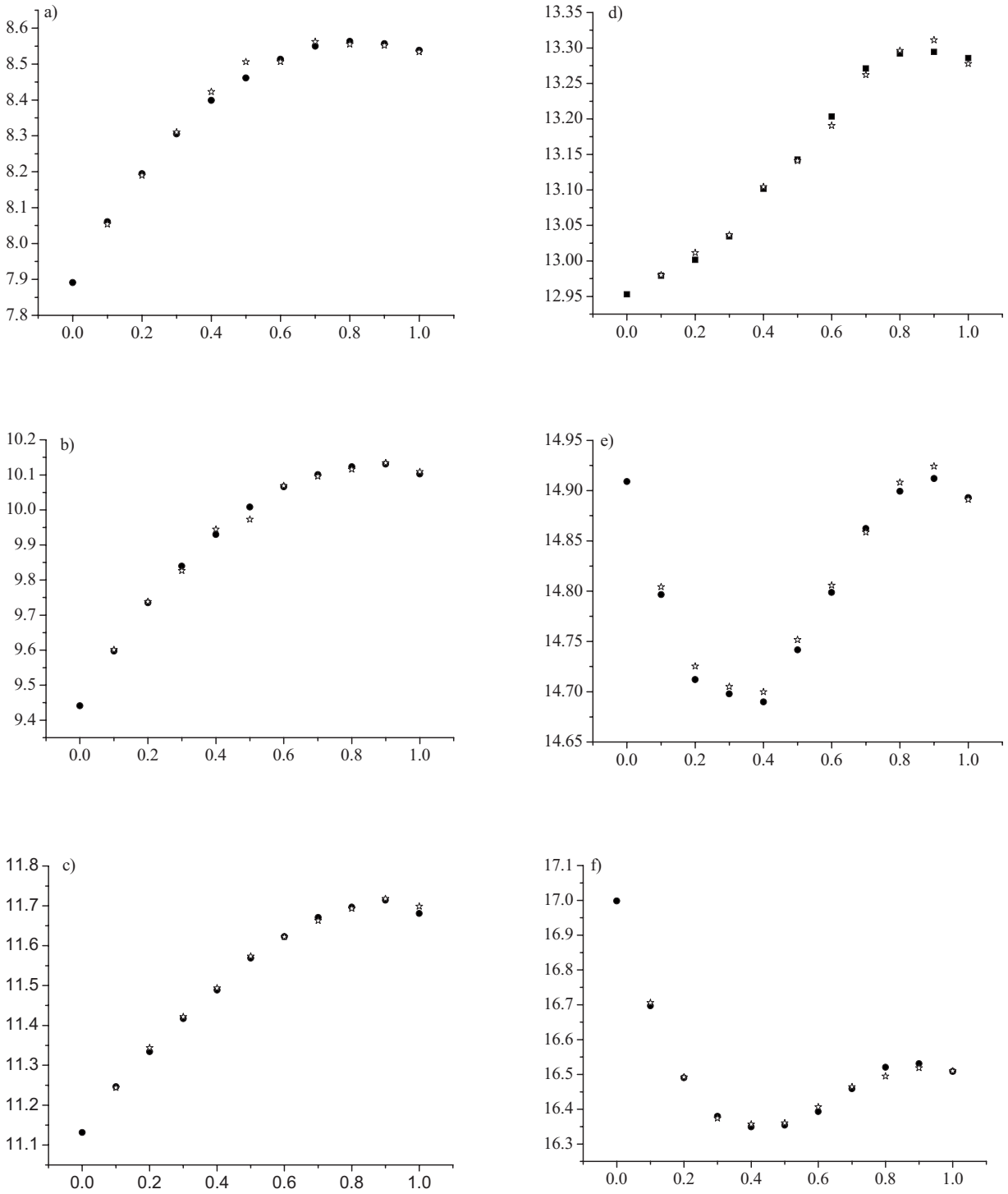

FIG. 12. $\langle\langle\tau\rangle\rangle_\rho$ vs ρ for different sizes $N=$ (a) 8, (b) 9, (c) 10, (d) 11, (e) 12, and (f) 13. Semianalytical results (dots) calculated from Eq. (25) with an ensemble of 10 000 network realizations and simulation results (stars) from 1000 random walks per initial site and 10 000 network realizations. We ascribe the slight discrepancies between the two sets of results to the finite number of random walk realizations and the strong N dependence of the MTA variance characteristic of first passage problems, resulting in nonsmooth numerical results. In general, the discrepancies tend to diminish with decreasing system size.

This is illustrated by the decrease of the local maximum of $\langle\langle\tau\rangle\rangle_\rho$ with increasing N; cf. Figs. 12(e) and 12(f).

Recently, Pandit and Amritkar [16] studied the trapping problem in SW networks of the Newmann-Watts type [18] (NWSW networks), with focus on the MTA for a walker initially placed at a distance m from the trap. The behavior of the MTA was analyzed as function of m, for different values of ρ. In particular, they calculated the AMTA for large networks in the limit $\rho \to 1$ by means of an effective field (EF) approach. Basically, this approach consists in exchanging the

averages in the definition of the AMTA, i.e., taking the average first over the network realizations and then over random walk realizations. The value of the AMTA in the limit $\rho \to 1$, obtained with the EF approach, has been reported to be equal to $N-1$ [16]. This result corresponds to the value of the AMTA obtained for Erdös-Rényi random networks [25] above the percolation critical threshold. In our case, the minimum value of $\langle\langle \tau \rangle\rangle_\rho$ is systematically higher than $N-1$. We do not expect this qualitative result to be different in the large size limit.

V. SUMMARY OF RESULTS

We have studied the effects arising from non-nearest-neighbor jumps, mobility of the trap, different absorption channels, and disorder in the network connections. Our Markov approach for periodic lattices relies both on recurrence relations and on the fundamental matrix approach, while the techniques used for the disordered case are based on the pseudoinverse of the Laplacian matrix. Recurrence relations have the advantage of being physically transparent and in principle easier to deal with than generating functions (as long as the degree of the associated characteristic polynomials remains small). A further advantage is that one can study a variety of trapping problems simply by slightly mutating the associated boundary conditions, including the case of nonzero mobility of the trap on a ring lattice [12] (in contrast, the method of generating functions requires dealing with a restricted random walk [14]). Our method allows one to straightforwardly compute the AMTA in terms of a scaling function containing detailed information about the dependence on both the system size and the control parameter for the walker-trap dynamics. The scaling function can then be used as a starting point to explore finite-size effects and the small-size limit relevant for nanotechnological applications.

In all cases, the emergence of nonmonotonic behavior can be basically understood as a competition between the effect of decreasing the effective system size on the one hand and enhancing the walker's delocalization on the other hand (for regular networks the latter effect is expected to become even more important in higher dimensions [26]). In periodic lattices, a single minimum of the AMTA as a function of the control parameter is seen for a proper parameter choice, while in the disordered case more complex behavior arises involving coexisting maxima and minima as a function of the disorder parameter ρ.

As we have seen, the competing effects at the origin of the optimization phenomena for trapping are universal in the sense that they subsist for different control parameters characterizing the walker-trap motion and interaction and the substrate geometry. However, we have also shown that the efficiency is very sensitive to specific details that should be taken into account for quantitative calculations.

ACKNOWLEDGMENTS

We are indebted to G. Nicolis for fruitful discussions and to the referee for helpful suggestions. A.G.C. thanks CONACyT for financial support. E.A. gratefully acknowledges financial support from the Wiener-Anspach Foundation.

[1] R. Pastor-Satorras and A. Vespignani, Phys. Rev. E **65**, 036104 (2002).
[2] Y. Moreno, M. Nekovee, and A. F. Pacheco, Phys. Rev. E **69**, 066130 (2004).
[3] E. W. Montroll, J. Math. Phys. **10**, 753 (1969).
[4] J. Whitmarsh and Govindjee, *Concepts in Photobiology: Photosynthesis and Photomorphogenesis* (Narosa, New Delhi, 1999).
[5] I. M. Sokolov, J. Mai, and A. Blumen, Phys. Rev. Lett. **79**, 857 (1997).
[6] J. Noolandi, Phys. Rev. B **16**, 4466 (1977).
[7] F. Fouss, A. Pirotte, J. M. Renders, and M. Saerens, IEEE Trans. Knowl. Data Eng. **19**, 355 (2007).
[8] M. Karlsson, M. Davidson, R. Karlsson, A. Karlsson, J. Bergenholtz, Z. Konkoli, A. Jesorka, T. Lobovkina, J. Hurtig, M. Voinova, and O. Orwar, Annu. Rev. Phys. Chem. **55**, 613 (2004).
[9] J. K. Gimzewski, Nova Acta Leopold. **17** (Suppl.), 29 (2001).
[10] J. G. Kemeny and J. L. Snell, *Finite Markov Chains* (Springer, New York, 1976).
[11] W. Feller, *An Introduction to Probability Theory and Its Applications I* (J. Wiley, New York, 1971).
[12] E. Abad, G. Nicolis, J. Bentz, and J. Kozak, Physica A **326**, 69 (2003).
[13] M. Coppey, O. Benichou, R. Voituriez, and M. Moreau, Biophys. J. **87**, 1640 (2004).
[14] E. Abad, Phys. Rev. E **72**, 021107 (2005).
[15] E. Almaas, R. V. Kulkarni, and D. Stroud, Phys. Rev. Lett. **88**, 098101 (2002).
[16] S. A. Pandit and R. E. Amritkar, Phys. Rev. E **63**, 041104 (2001).
[17] P. E. Parris and V. M. Kenkre, Phys. Rev. E **72**, 056119 (2005).
[18] M. E. J. Newman, C. Moore, and D. J. Watts, Phys. Rev. Lett. **84**, 3201 (2000).
[19] D. J. Watts and S. H. Strogatz, Nature (London) **393**, 440 (1998).
[20] C. Jordan, *Calculus of Finite Differences* (Chelsea, New York, 1979).
[21] K. Lakatos-Lindenberg and K. E. Schuler, J. Math. Phys. **12**, 633 (1971).
[22] J. L. Bentz, J. J. Kozak, and G. Nicolis, Physica A **353**, 73 (2005).
[23] J. M. Zimann, *Models of disorder* (Cambridge University Press, Cambridge, U.K., 1979).
[24] A. Ben-Israel and T. Grenville, *Generalized Inverses: Theory and applications*, 2nd ed. (Springer, New York, 2003).
[25] V. Sood, S. Redner and D. ben-Avraham, J. Phys. A **38**, 109 (2005).
[26] E. Abad and J. J. Kozak, Physica A **370**, 501 (2006).